

## Chapter 4

# Approximate analytical solution of coupled fractional order reaction-advection-diffusion equations

### 4.1 Introduction

This chapter contains the study and analysis of time-fractional non-linear coupled reaction-advection-diffusion equations with prescribed Dirichlet initial and boundary conditions. The study of system of coupled PDEs has been spreaded widely in bio-mathematics, engineering and other fields. Coupled systems of FPDEs appear in the modeling of many important gravitational and electromagnetic problems [88, 89]. The various applications of coupled PDEs can be found in mechanics and solid state physics [90, 91]. The study of system of PDEs is also found in the modeling the problems in biomechanics during electrical activity in heart [92].

In literature, a wide spreaded uses of FPDEs to model many physical and chemical phenomena, for instance, fluid flow of tracers through porous media and fluid diffusion in porous media [93, 94, 95] are found. The authors of [82, 96, 97, 98] have used the concept of fractional order derivatives to describe the behaviors of fluid flow in porous media. But to the best of author's knowledge the solution of a system of fractional order nonlinear coupled equations in porous media is first of its kind.

In this chapter, a physical problem is modeled into a mathematical problem. Two crucial solute variables are considered which describe the two interacting species of the nature influenced under the convection and diffusion in fluid flow through porous medium. There is a lot of challenging factors like transient nature, coupling and non-linearity of the model which make it one of the most complex physical systems to deal it analytically or numerically. It is considered that two reacting species interact with each other and diffuse from higher concentration to lower concentration. The main accentuation of the model is to analyze the long term characterization of the system. Here a system of two fractional order nonlinear reaction-advection-diffusion equation in one space dimension is considered subject to Dirichlet initial and boundary conditions. The concerned system of coupled FPDEs contains mixed partial derivatives in the Caputo sense [64, 65] with respect to  $x, t$  as given by

$$\begin{aligned}\frac{\partial^{\alpha_1} u}{\partial t^{\alpha_1}} &= a_1 \frac{\partial^2 u}{\partial x^2} + a_2 u^m \frac{\partial u}{\partial x} - a_3 \frac{\partial(uv)}{\partial x} + k_1 u(1-u), \\ \frac{\partial^{\alpha_2} v}{\partial t^{\alpha_2}} &= b_1 \frac{\partial^2 v}{\partial x^2} + b_2 v^n \frac{\partial v}{\partial x} - b_3 \frac{\partial(uv)}{\partial x} + k_2 v(1-v),\end{aligned}\quad (4.1)$$

corresponding to the initial and boundary conditions

$$u(x, 0) = l_1(x), \quad u(0, t) = m_1(t), \quad u(1, t) = n_1(t), \quad (4.2)$$

$$v(x, 0) = l_2(x), \quad v(0, t) = m_2(t), \quad v(1, t) = n_2(t), \quad (4.3)$$

where  $m, n, a_i$ 's and  $b_i$ 's are the arbitrary constants.  $k_1$  and  $k_2$  are the diffusion coefficients for the species  $u$  and  $v$  respectively,  $\alpha_1, \alpha_2$  are fractional order derivatives s.t.  $0 < \alpha_1, \alpha_2 < 1$ .

Some particular cases of above concerned model have been found in various physical phenomena as discussed in [99, 100]. For some suitable values of arbitrary constants, the concerned model is converted into well known Burgers' equations. The system of coupled Burgers' equations mainly describes the physical behavior of evolution or sedimentation of concentration of two species under the effect of gravity during the fluid colloids or suspension phenomenon [101]. The coupled systems of Burgers' equations had been derived by Esipov [102]. Many researchers have developed several numerical schemes to encounter the Burgers' equations. The commonly used approach for Burgers' equation is Cole-Hopf transformation [103]. The solution of Burgers' equation by the symmetry reduction method is found in terms of Airy functions or parabolic cylinder functions.

The aim of this chapter is to propose one of the powerful and efficient techniques viz., Laguerre collocation method to get the approximate solutions for the concerned nonlinear FPDEs with initial and boundary conditions. The main reason behind using this powerful and efficient method is its higher order of convergence even at very small number of grids approximation. Operational matrix based on Laguerre collocation method is very efficient and reliable because of the orthogonality of Laguerre polynomials. Among other numerical techniques, Laguerre collocation method is efficient tool to approximate and handling the various PDEs. A truncated orthogonal series based on Laguerre polynomial is a powerful tool to solve NFPDEs in higher order of accuracy on a simple domain. To apply the collocation technique, the role of choosing a collocation point is very significant for efficiency and convergence of the collocation approximation as it converts the concerned model into a nonlinear system of algebraic equations which are further solved by using Newton's iterative method. The super-linearity of the convergence rate of our proposed method is authenticated through one considered text example for both temporal and spatial discretizations. In order to show the accuracy and efficiency of the proposed method, it has been applied to a complex physical problem. Comparison of the approximate solution with the existing analytical solution is shown through the graphical forms and in tabular forms as well.

Generally in the case of two solute particles, the study of diffusion for each species becomes extremely complicated. But in the present endeavor, diffusion of each species of the concerned model is more easily explained through the pictorial presentations of the solution profile for different particular cases. The interactions between the solute and solvent affect the diffusions of solute profiles. For the case of conservative system i.e., in the absence of reaction term, both the solute species diffuse faster as compared to the diffusion in sink term. It should be also noticed that, the solute profile diffuses faster for the case of fractional order system as compared to the integer order system, which justifies the importance of fractional order system over an integer order system.

## 4.2 Laguerre operational matrix for fractional order derivatives

The definition of Laguerre polynomials and its some properties are discussed in section (2.3) of Chapter 2. The operational matrix for fractional order derivative of order  $\alpha$  is

constructed in Theorem 2.2 of Chapter 2. We can write it as

$$G^{(\alpha)} = \begin{bmatrix} 0 & 0 & 0 & \dots & 0 \\ \vdots & \vdots & \vdots & \dots & \vdots \\ 0 & 0 & 0 & \dots & 0 \\ S_{\alpha}([\alpha], 0) & S_{\alpha}([\alpha], 1) & S_{\alpha}([\alpha], 2) & \dots & S_{\alpha}([\alpha], N) \\ \vdots & \vdots & \vdots & \dots & \vdots \\ S_{\alpha}(i, 0) & S_{\alpha}(i, 1) & S_{\alpha}(i, 2) & \dots & S_{\alpha}(i, N) \\ \vdots & \vdots & \vdots & \dots & \vdots \\ S_{\alpha}(N, 0) & S_{\alpha}(N, 1) & S_{\alpha}(N, 2) & \dots & S_{\alpha}(N, N) \end{bmatrix}. \quad (4.4)$$

### 4.3 The method proposed for Laguerre operational matrix of fractional order derivatives

In this section of the chapter, the main goal is to propose the collocation method in a suitable way based on Laguerre operational matrix so that the method can be implemented efficiently to solve the concerned model.

Now,  $u(x, t)$  and  $v(x, t)$  are approximated in forms of Laguerre polynomials as

$$u(x, t) = \sum_{a=0}^N \sum_{b=0}^N c_{ab} L_a(x) L_b(t), \quad v(x, t) = \sum_{l=0}^N \sum_{m=0}^N c'_{lm} L_l(x) L_m(t), \quad (4.5)$$

where  $c_{ab}$  and  $c'_{lm}$ , the unknown coefficients, which will be calculated later for  $a, b, l, m = 1, 2, 3, \dots$ ; The equation (4.5) can be rewritten in matrix form as

$$u(x, t) = \phi^T(x) \cdot C \cdot \phi(t), \quad v(x, t) = \phi^T(x) \cdot C' \cdot \phi(t), \quad (4.6)$$

where  $C = [c_{ab}]$  and  $C' = [c'_{lm}]$  are matrices of order  $(N + 1) \times (N + 1)$  of arbitrary unknown constant coefficients and  $\phi(t) = (L_0(t), L_1(t), \dots, L_N(t))^T$  is a column vector.

Now, using fractional differentiation of order  $\alpha, \beta$  with respect to  $t, x$  respectively on the equation (4.6) and using Theorem 2.2 of Chapter 2, we get

$$\left. \begin{aligned} \frac{\partial^{\alpha} u}{\partial t^{\alpha}} &= D^{\alpha} u(x, t) = \phi^T(x) \cdot C \cdot D^{\alpha} \phi(t), \\ \frac{\partial^{\alpha} v}{\partial t^{\alpha}} &= D^{\alpha} v(x, t) = \phi^T(x) \cdot C' \cdot D^{\alpha} \phi(t), \end{aligned} \right\} \quad (4.7)$$

and

$$\left. \begin{aligned} \frac{\partial^\beta u}{\partial x^\beta} &= D^\beta u(x, t) = D^\beta \phi^T(x) \cdot C \cdot \phi(t), \\ \frac{\partial^\beta v}{\partial x^\beta} &= D^\beta v(x, t) = D^\beta \phi^T(x) \cdot C' \cdot \phi(t). \end{aligned} \right\} \quad (4.8)$$

Now from boundary conditions (4.2)-(4.3) with the aid of equation (4.6), we get

$$\phi^T(x) \cdot C \cdot \phi(0) = x^2, \quad \phi^T(0) \cdot C \cdot \phi(t) = t^2, \quad \phi^T(1) \cdot C \cdot \phi(t) = 1 + t^2, \quad (4.9)$$

$$\phi^T(x) \cdot C' \cdot \phi(0) = x^2, \quad \phi^T(0) \cdot C' \cdot \phi(t) = t^2, \quad \phi^T(1) \cdot C' \cdot \phi(t) = 1 + t^2. \quad (4.10)$$

Now let us collocate equation (4.1) with the help of equations (4.9) and (4.10) at points  $x_a = \frac{a}{N}$  for  $a = 0, 1, 2, \dots, N$  and  $t_a = \frac{a}{N}$  for  $a = 0, 1, 2, \dots, N$ .

After collocating, we get a system of non-linear equations. Further by simplifying this non-linear algebraic system of equations and finding  $C$  and  $C'$ , we obtain numerical solution of the given problem by substituting  $C$  and  $C'$  in equation (4.6).

#### 4.4 Convergence analysis of the proposed approximation

The special attention is given in this section to estimate upper bound of the error of proposed approximation. The main attention is focused on whether solution of the proposed fractional order mathematical model obtained by applying the approximate numerical scheme converges to the exact solution or not. Convergence will be assured by showing the error obtained through approximating  $(\frac{\partial^\alpha u}{\partial t^\alpha})$  and  $(\frac{\partial^\alpha v}{\partial t^\alpha})$  by  $(\frac{\partial^\alpha u}{\partial t^\alpha})_N$  and  $(\frac{\partial^\alpha v}{\partial t^\alpha})_N$ , respectively in terms of orthogonal Laguerre polynomials is bounded in magnitude by some bounds. Here some theorems and remarks are provided before the proof of the main theorem.

**Theorem 4.1.** *Suppose  $u(x, t)$  and  $v(x, t)$  be the sufficiently smooth functions on the region  $A$ ,  $(\frac{\partial^\alpha u}{\partial t^\alpha})_N$  and  $(\frac{\partial^\alpha v}{\partial t^\alpha})_N$  be the approximations of  $(\frac{\partial^\alpha u}{\partial t^\alpha})$  and  $(\frac{\partial^\alpha v}{\partial t^\alpha})$  respectively. Then the errors in approximating  $(\frac{\partial^\alpha u}{\partial t^\alpha})$ ,  $(\frac{\partial^\alpha v}{\partial t^\alpha})$  by  $(\frac{\partial^\alpha u}{\partial t^\alpha})_N$  and  $(\frac{\partial^\alpha v}{\partial t^\alpha})_N$  respectively are bounded by*

$$|E_r(N)| \leq \sum_{a=N+1}^{\infty} \sum_{b=N+1}^{\infty} \frac{c_{ab}}{a! \cdot m!} \chi_{mbN} e^{\frac{x+t}{2}}, \quad x, t \geq 0, \quad a, b = 0, 1, 2, \dots; \quad (4.11)$$

and

$$| E_r'(N) | \leq \sum_{h=N+1}^{\infty} \sum_{k=N+1}^{\infty} \frac{c'_{hk}}{h! \cdot m!} \chi_{mkN} e^{\frac{x+t}{2}}, \quad x, t \geq 0, \quad h, k = 0, 1, 2, \dots, \quad (4.12)$$

where  $\chi_{mbN} = \sum_{m=0}^N S_{\alpha}(b, m)$  and  $\chi_{mkN} = \sum_{m=0}^N S_{\alpha}(k, m)$ .

**Proof.** In view of the equation (4.5), we have

$$u(x, t) = \sum_{a=0}^{\infty} \sum_{b=0}^{\infty} c_{ab} L_a(x) L_b(t), \quad v(x, t) = \sum_{h=0}^{\infty} \sum_{k=0}^{\infty} c'_{hk} L_h(x) L_k(t). \quad (4.13)$$

Truncating upto  $N + 1$  terms, we have

$$u_N(x, t) = \sum_{a=0}^N \sum_{b=0}^N c_{ab} L_a(x) L_b(t), \quad v_N(x, t) = \sum_{h=0}^N \sum_{k=0}^N c'_{hk} L_h(x) L_k(t). \quad (4.14)$$

We can write  $\alpha$  order partial derivatives of  $u(x, t)$  and  $u_N(x, t)$  w.r.to  $t$  as

$$\frac{\partial^{\alpha} u}{\partial t^{\alpha}} = \sum_{a=0}^{\infty} \sum_{b=0}^{\infty} c_{ab} L_a(x) \frac{\partial^{\alpha} L_b(t)}{\partial t^{\alpha}}, \quad \left( \frac{\partial^{\alpha} u}{\partial t^{\alpha}} \right)_N = \sum_{a=0}^N \sum_{b=0}^N c_{ab} L_a(x) \frac{\partial^{\alpha} L_b(t)}{\partial t^{\alpha}}. \quad (4.15)$$

From the above equations, we can write

$$E_r(N) = \frac{\partial^{\alpha} u}{\partial t^{\alpha}} - \left( \frac{\partial^{\alpha} u}{\partial t^{\alpha}} \right)_N = \sum_{a=N+1}^{\infty} \sum_{b=N+1}^{\infty} c_{ab} L_a(x) \frac{\partial^{\alpha} L_b(t)}{\partial t^{\alpha}}. \quad (4.16)$$

Using the equation (2.30) of Chapter 2, the above expression reduces to

$$| E_r(N) | = \left| \sum_{a=N+1}^{\infty} \sum_{b=N+1}^{\infty} c_{ab} L_a(x) \left( \sum_{m=0}^N S_{\alpha}(b, m) L_m(t) \right) \right|, \quad (4.17)$$

or,

$$| E_r(N) | = \sum_{a=N+1}^{\infty} \sum_{b=N+1}^{\infty} c_{ab} \cdot \chi_{mbN} | L_m(t) | \cdot | L_a(t) |. \quad (4.18)$$

Applying equation (2.42) of Chapter 2, we get

$$| E_r(N) | \leq \sum_{a=N+1}^{\infty} \sum_{b=N+1}^{\infty} c_{ab} \cdot \chi_{mbN} \cdot \frac{1}{m!} e^{\frac{t}{2}} \cdot \frac{1}{a!} e^{\frac{x}{2}}, \quad (4.19)$$

or,

$$|E_r(N)| \leq \sum_{a=N+1}^{\infty} \sum_{b=N+1}^{\infty} \frac{c_{ab}}{a! \cdot m!} \chi_{mbN} e^{\frac{x+t}{2}}, \quad x, t \geq 0, \quad a, b = 0, 1, 2, \dots; \quad (4.20)$$

Thus we have the required proof. Similarly, we can prove the second part of the theorem. Therefore error of approximation is bounded and thus the convergence of approximation is assured.  $\square$

## 4.5 Error analysis and accuracy of the method

In this section Laguerre polynomial operational matrix method of the fractional order derivatives has been applied for the solutions of some existing fractional order coupled partial differential equations and compare the obtained results with their analytical solutions through absolute error formula to illustrate the accuracy and efficiency of the proposed scheme. All the numerical computations are carried out by using MATHEMATICA 11.3.

The absolute error calculated for the different existing problems is defined as

$$E_{abs}(x, t) = |u_{exact}(x, t) - u_{num}(x, t)|. \quad (4.21)$$

Maximum error for the problem in  $x$  for fixed  $t$  is defined as

$$MaxE_{abs}(x, 0.5) = \max_{0 \leq x \leq 1} |E_{abs}(x, 0.5)|. \quad (4.22)$$

Similarly, maximum error for the problem in  $t$  for fixed  $x$  is defined as

$$MaxE_{abs}(0.5, t) = \max_{0 \leq t \leq 1} |E_{abs}(0.5, t)|. \quad (4.23)$$

In addition, to show the higher order accuracy of the proposed model let us define the order of convergence for two successive approximations  $N_1$  and  $N_2$  as

$$Order = \frac{\log\left(\frac{MaxE_{abs}(N_1)}{MaxE_{abs}(N_2)}\right)}{\log\left(\frac{N_2}{N_1}\right)}, \quad (4.24)$$

where  $MaxE_{abs}(N)$  is the maximum absolute error for the approximation of degree  $N$ .

During validation of the efficiency of the proposed numerical scheme compared to other existing numerical methods, the following two types of errors known as  $L_2$  and  $L_\infty$  norms for continuous domain with fix value of  $t$  are used, which are defined by

$$\|u_{exact} - u_{num}\|_{L_2} = \sqrt{\int_0^1 |u_{exact}(x, t_1) - u_{num}(x, t_1)|^2 dx}, \quad (4.25)$$

$$\|u_{exact} - u_{num}\|_{L_\infty} = \max_{0 \leq x \leq 1} |u_{exact}(x, t_1) - u_{num}(x, t_1)|. \quad (4.26)$$

**Example 1:** Let us consider the proposed model for the case  $\alpha_1 = \alpha_2 = a_1 = a_3 = b_1 = b_3 = m = n = 1, a_2 = b_2 = 2$  and  $k_1 = 0 = k_2$ , then equations (4.1) are reduced to

$$\begin{aligned} \frac{\partial u}{\partial t} &= \frac{\partial^2 u}{\partial x^2} + 2u \frac{\partial u}{\partial x} - \frac{\partial(uv)}{\partial x}, \\ \frac{\partial v}{\partial t} &= \frac{\partial^2 v}{\partial x^2} + 2v \frac{\partial v}{\partial x} - \frac{\partial(uv)}{\partial x}, \end{aligned} \quad (4.27)$$

with  $l_1(x) = \sin x$ ,  $m_1(t) = 0$ ,  $n_1(t) = \frac{\sin(1)}{\exp(t)}$ ,  $l_2(x) = \sin x$ ,  $m_2(t) = 0$ , and  $n_2(t) = \frac{\sin(1)}{\exp(t)}$ . The reduced system of coupled nonlinear PDEs under the mentioned initial and boundary conditions is well known coupled Burgers' equations with exact solutions as  $u(x, t) = \exp(-t) \sin(x), v(x, t) = \exp(-t) \sin(x)$ . The error analysis and order of convergence are exhibited through Table 4.1 and Table 4.2 for  $t = 0.5, 0 \leq x \leq 1$  for the order of approximation  $N = 3, 4, 5, 6$ . The tables clearly confirm that the order of convergence of the proposed method increases as the degree of Laguerre polynomials in  $x$  increases. Again the absolute error decreases with the increase of the order of approximation of the polynomial  $N$ , which clearly shows the effectiveness of the proposed numerical method. Again the data of CPU time shows that it takes minimum time to obtain accurate result which shows the method is computationally effective to solve coupled systems of NPDEs.

TABLE 4.1: Efficiency of the numerical method for  $u(x, t)$  at  $t=0.5$

t	N	Maximal absolute error $0 \leq x \leq 1$	Order of convergence	CPU Time (second)
0.5	3	$3.21 \times 10^{-4}$	-	09.263
	4	$3.58 \times 10^{-5}$	7.62	11.361
	5	$1.51 \times 10^{-6}$	14.18	13.048
	6	$1.00 \times 10^{-7}$	14.89	14.374

TABLE 4.2: Efficiency of the numerical method for  $v(x, t)$  at  $t=0.5$ 

t	N	Maximal absolute error $0 \leq x \leq 1$	Order of convergence	CPU Time (second)
0.5	3	$3.21 \times 10^{-4}$	-	09.263
	4	$3.58 \times 10^{-5}$	7.62	11.361
	5	$1.51 \times 10^{-6}$	14.18	13.048
	6	$9.81 \times 10^{-8}$	14.99	14.374

The absolute errors between the exact solution and the numerical solution are shown through Fig. 4.1 and Fig. 4.2 for various values of  $x$  and  $t$ . Fig. 4.1 and Fig. 4.2 show that the numerical solutions of  $u(x, t)$  and  $v(x, t)$  are approximately accurate to the exact solutions even for smaller value  $N = 6$ . The better convergence can be achieved with the increase in  $N$ . Thus comparing the numerical solution with the exact solution, it can be said that the proposed method is very much efficient.

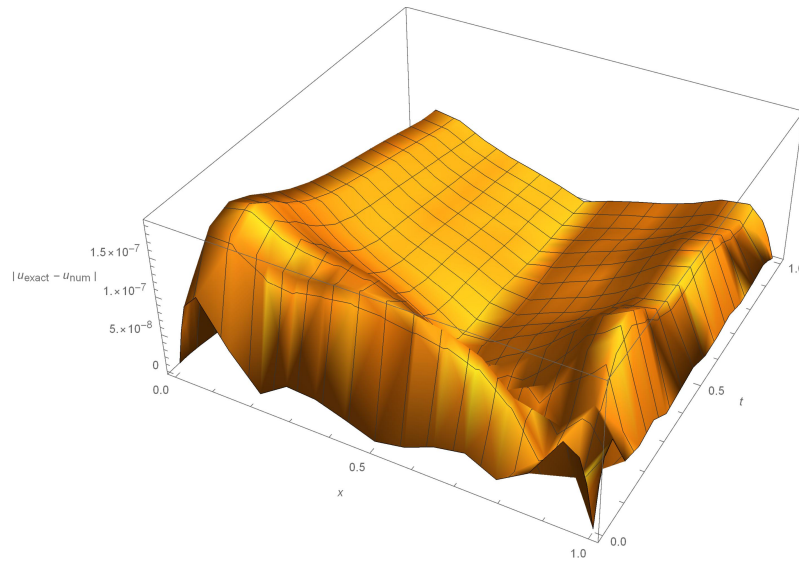


FIGURE 4.1: Plot of the absolute error between the exact and numerical solutions of  $u(x, t)$  vs.  $x$  and  $t$  for  $N = 6$

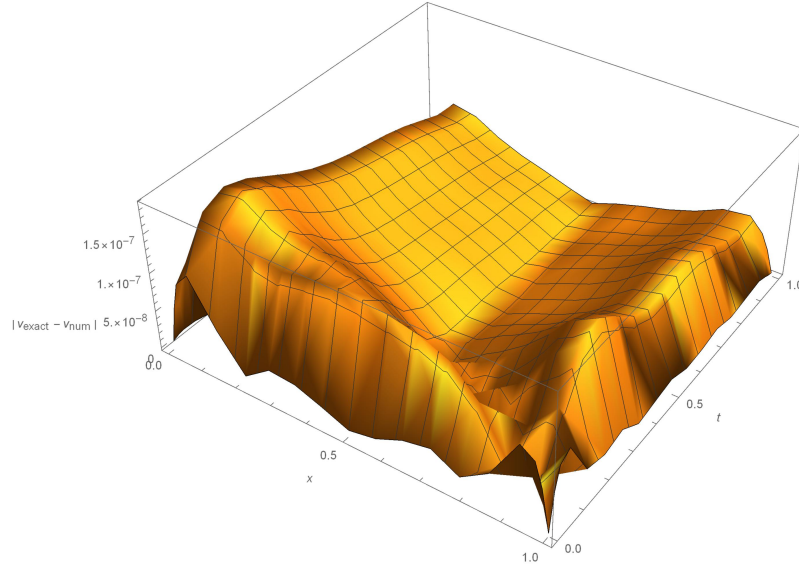


FIGURE 4.2: Plot of the absolute error between the exact and numerical solutions of  $v(x, t)$  vs.  $x$  and  $t$  for  $N = 6$

The numerical computation errors  $L_2$  (root mean square error) and  $L_\infty$  (maximum absolute error) of concerned Example 1 for different values of  $t$  for both  $u(x, t)$  and  $v(x, t)$  obtained by the numerical scheme (for  $N = 6$ ) and the method given in [104] are shown through Tables 4.3-4.4. It is seen from the tables that the proposed scheme is more accurate as compared to the method given in [104].

TABLE 4.3: Comparison of  $L_2$  and  $L_\infty$  errors for  $u(x, t)$  for different values of  $t$

t	Proposed method		Mittal et al. [104]	
	$L_2$	$L_\infty$	$L_2$	$L_\infty$
0.01	$5.62 \times 10^{-8}$	$1.13 \times 10^{-7}$	$3.49 \times 10^{-4}$	$2.90 \times 10^{-4}$
0.1	$1.38 \times 10^{-7}$	$1.89 \times 10^{-7}$	$3.78 \times 10^{-4}$	$2.65 \times 10^{-4}$
0.5	$6.62 \times 10^{-8}$	$1.19 \times 10^{-7}$	$4.47 \times 10^{-4}$	$1.07 \times 10^{-4}$
1	$4.22 \times 10^{-8}$	$7.07 \times 10^{-8}$	$7.87 \times 10^{-4}$	$3.76 \times 10^{-4}$

TABLE 4.4: Comparison of  $L_2$  and  $L_\infty$  errors for  $v(x, t)$  for different values of  $t$ 

t	Proposed method		Mittal et al. [104]	
	$L_2$	$L_\infty$	$L_2$	$L_\infty$
0.01	$5.49 \times 10^{-8}$	$1.12 \times 10^{-7}$	$3.49 \times 10^{-4}$	$2.90 \times 10^{-4}$
0.1	$1.30 \times 10^{-7}$	$1.89 \times 10^{-7}$	$3.78 \times 10^{-4}$	$2.65 \times 10^{-4}$
0.5	$6.59 \times 10^{-8}$	$1.19 \times 10^{-7}$	$4.47 \times 10^{-4}$	$1.07 \times 10^{-4}$
1	$4.21 \times 10^{-8}$	$7.07 \times 10^{-8}$	$7.87 \times 10^{-4}$	$3.76 \times 10^{-4}$

**Example 2:** Let us consider our proposed model for the case  $\alpha_1 = \alpha_2 = a_1 = b_1 = m = n = 1, a_2 = b_2 = 2, a_3 = 0.1, b_3 = 0.3$  and  $k_1 = 0 = k_2$ . The equations (4.1) are reduced to

$$\begin{aligned}\frac{\partial u}{\partial t} &= \frac{\partial^2 u}{\partial x^2} + 2u \frac{\partial u}{\partial x} - 0.1 \frac{\partial(uv)}{\partial x}, \\ \frac{\partial v}{\partial t} &= \frac{\partial^2 v}{\partial x^2} + 2v \frac{\partial v}{\partial x} - 0.3 \frac{\partial(uv)}{\partial x},\end{aligned}\quad (4.28)$$

whose exact solutions are given by

$$\begin{aligned}u(x, t) &= b_0(1 - \tanh(B(20(x - 0.5) - 2Bt))), \\ v(x, t) &= b_0\left(\left(\frac{2b_3 - 1}{2a_3 - 1}\right) - \tanh(B(20(x - 0.5) - 2Bt))\right),\end{aligned}\quad (4.29)$$

where  $b_0 = 0.05, B = (1/2)b_0\left(\frac{4a_3b_3-1}{2a_3-1}\right)$  under the boundary conditions  $u(x, 0) = b_0(1 - \tanh(B(20(x - 0.5))))$ ,  $u(0, t) = b_0(1 - \tanh(B(20(-0.5) - 2Bt))$ ,  $u(1, t) = b_0(1 - \tanh(B(20(0.5) - 2Bt))$ ,  $v(x, 0) = b_0\left(\left(\frac{2b_3-1}{2a_3-1}\right) - \tanh(B(20(x - 0.5)))\right)$ ,  $v(0, t) = b_0\left(\left(\frac{2b_3-1}{2a_3-1}\right) - \tanh(B(20(-0.5) - 2Bt))\right)$  and  $v(1, t) = b_0\left(\left(\frac{2b_3-1}{2a_3-1}\right) - \tanh(B(20(0.5) - 2Bt))\right)$ .

For this problem the  $L_2$  and  $L_\infty$  errors for  $u(x, t)$  and  $v(x, t)$  are tabulated in Table 4.5 and Table 4.6, respectively for our numerical scheme and also for the numerical method given in [105] obtained by using Chebyshev wavelets. Here also it is found that the proposed numerical method is much superior as compared to the method given in [105].

TABLE 4.5: Comparison of  $L_2$  and  $L_\infty$  errors for  $u(x, t)$  for different values of  $t$ 

t	Proposed method		Method given in [105]		CPU Time (second)
	$L_2$	$L_\infty$	$L_2$	$L_\infty$	
1	$2.59 \times 10^{-5}$	$3.96 \times 10^{-5}$	$1.33 \times 10^{-3}$	$8.21 \times 10^{-5}$	09.301
0.5	$2.53 \times 10^{-6}$	$3.88 \times 10^{-5}$	$6.79 \times 10^{-4}$	$4.15 \times 10^{-5}$	09.361

TABLE 4.6: Comparison of  $L_2$  and  $L_\infty$  errors for  $v(x, t)$  for different values of  $t$ 

t	Proposed method		Method given in [105]		CPU Time (second)
	$L_2$	$L_\infty$	$L_2$	$L_\infty$	
1	$1.25 \times 10^{-6}$	$2.10 \times 10^{-5}$	$9.85 \times 10^{-4}$	$4.12 \times 10^{-5}$	09.297
0.5	$1.21 \times 10^{-6}$	$2.04 \times 10^{-6}$	$2.03 \times 10^{-4}$	$9.39 \times 10^{-6}$	09.315

## 4.6 Results and discussion for proposed model

After being a justification of the accuracy and effectiveness of the method, the author has been motivated to solve the proposed system of coupled fractional order partial differential equations (4.1) with the initial and boundary conditions (4.2) – (4.3). The variations of the solute concentrations  $u(x, t)$  and  $v(x, t)$  vs. the column length  $x$  at  $t = 0.5$  for different values of the fractional order time parameters  $\alpha_1, \alpha_2$  for non-conservative case ( $k = 1, -1$ ) are calculated numerically, which have been presented graphically through Figs. 4.3-4.8.

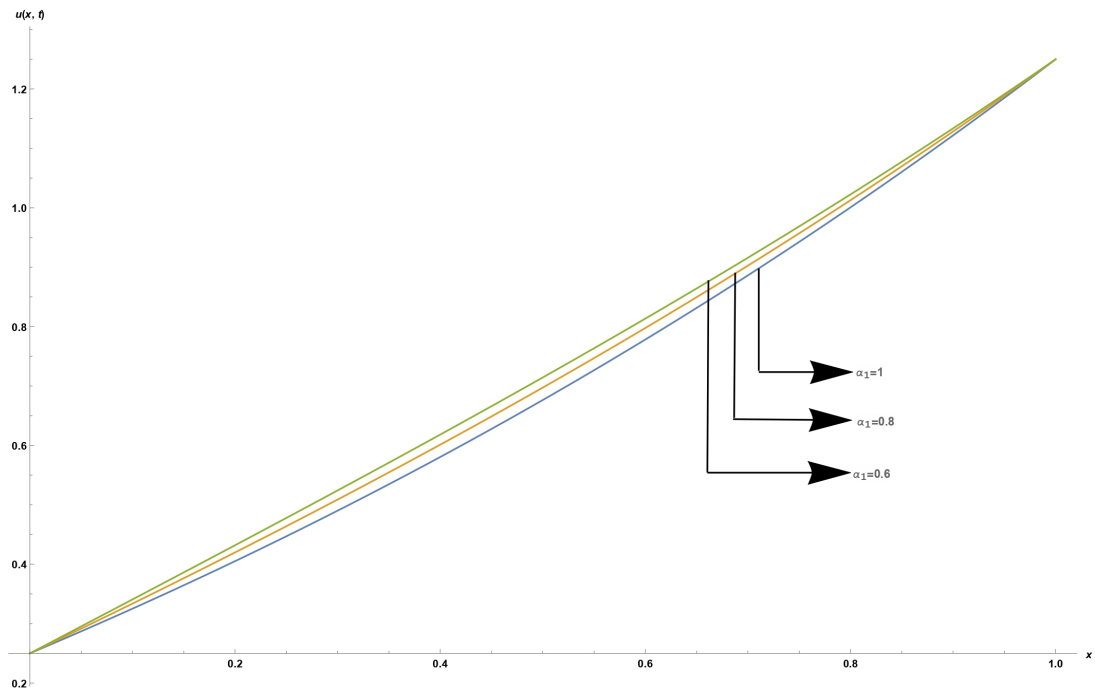


FIGURE 4.3: Plots of the solute concentration  $u(x, t)$  vs.  $x$  for different values of  $\alpha_1$  for  $k_1 = k_2 = 1, \alpha_2 = 1$  at  $t = 0.5$ .

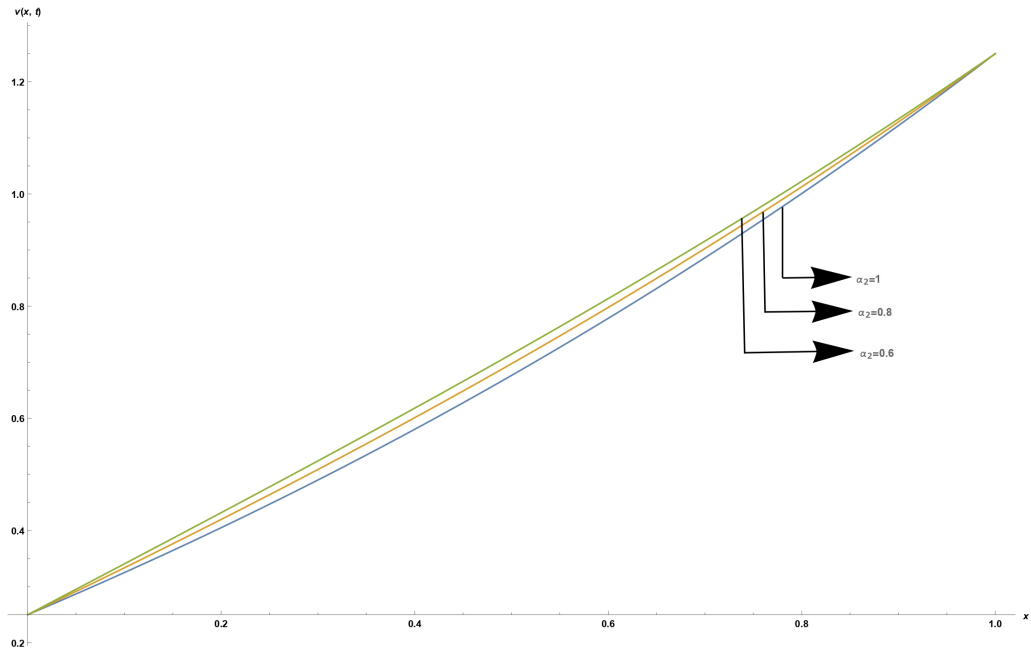


FIGURE 4.4: Plots of the solute concentration  $v(x, t)$  vs.  $x$  for different values of  $\alpha_2$  for  $k_1 = k_2 = 1, \alpha_1 = 1$  at  $t = 0.5$ .

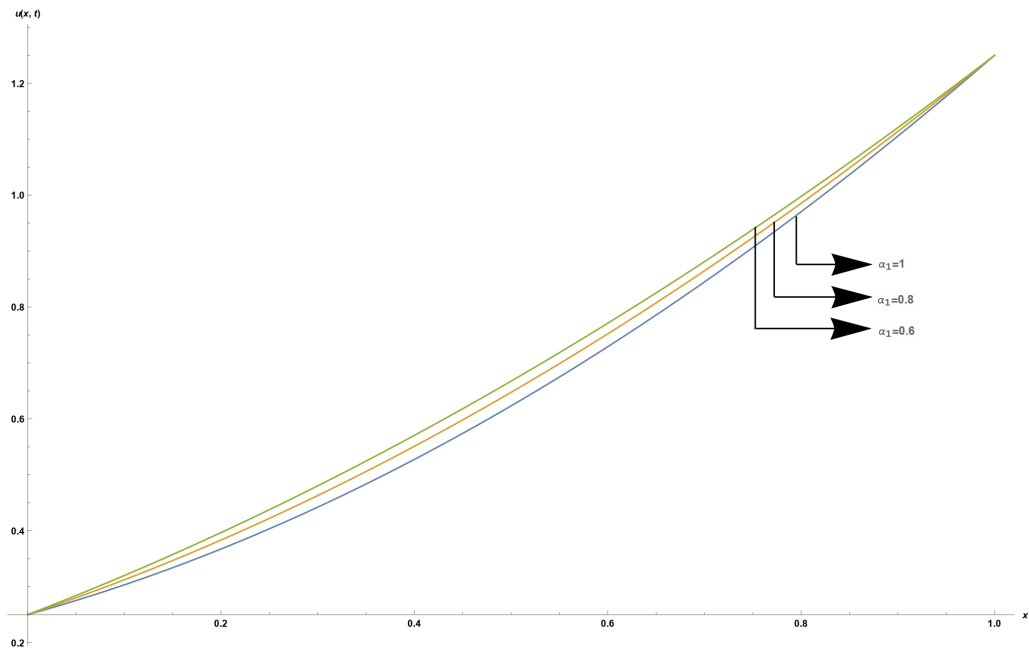


FIGURE 4.5: Plots of the solute concentration  $u(x, t)$  vs.  $x$  for different values of  $\alpha_1$  for  $k_1 = k_2 = -1, \alpha_2 = 1$  at  $t = 0.5$ .

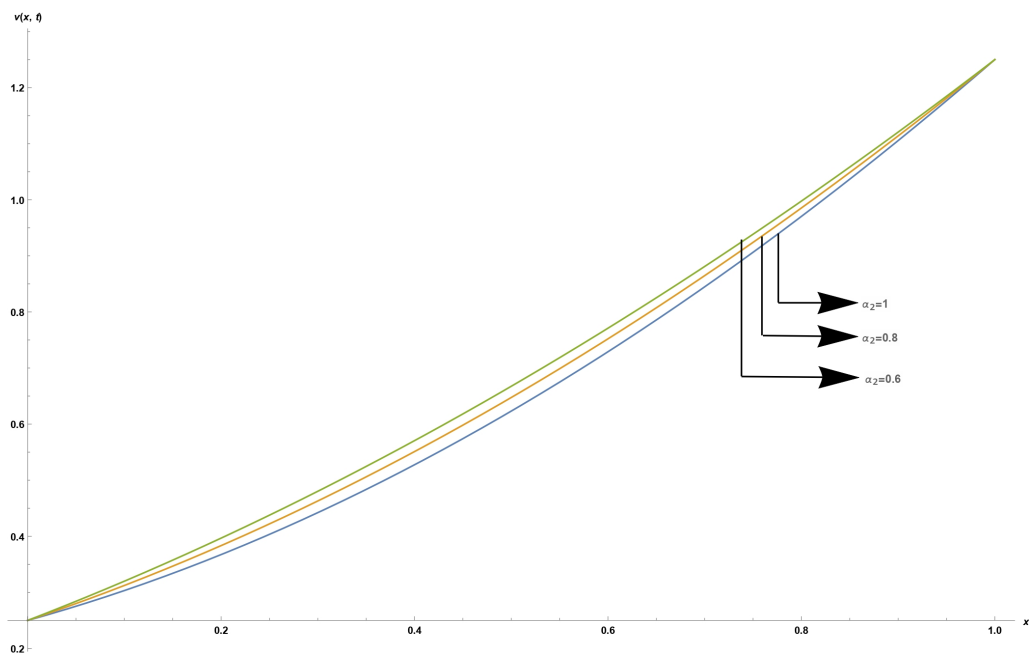


FIGURE 4.6: Plots of the solute concentration  $v(x, t)$  vs.  $x$  for different values of  $\alpha_2$  for  $k_1 = k_2 = -1, \alpha_1 = 1$  at  $t = 0.5$ .

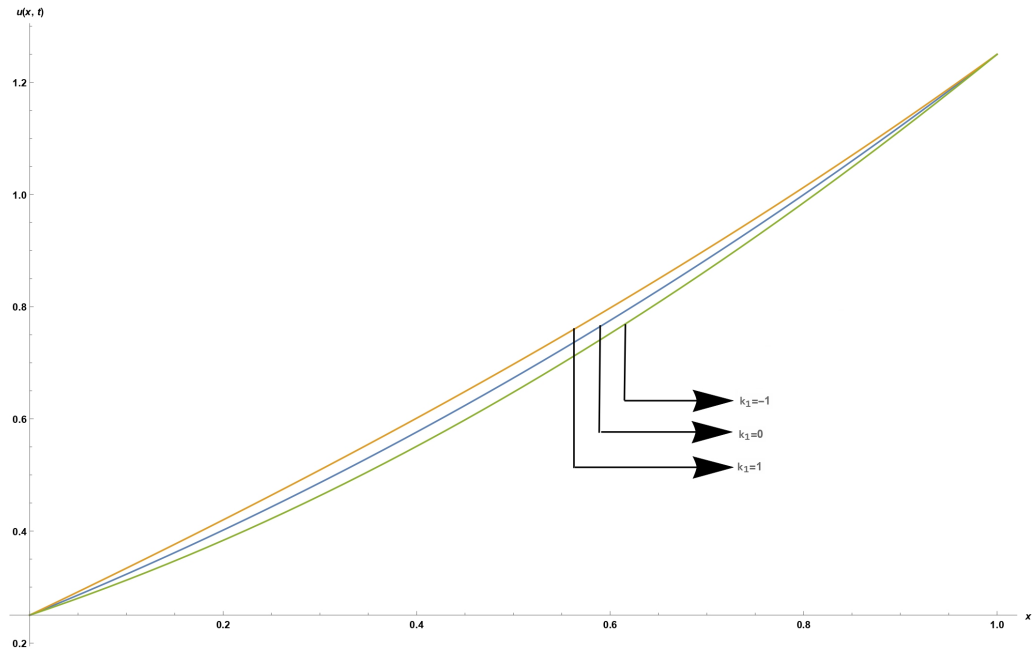


FIGURE 4.7: Plots of the solute concentration  $u(x, t)$  vs.  $x$  for different values of  $k_1$  for  $\alpha_1 = 0.8, \alpha_2 = 1$  at  $t = 0.5$ .

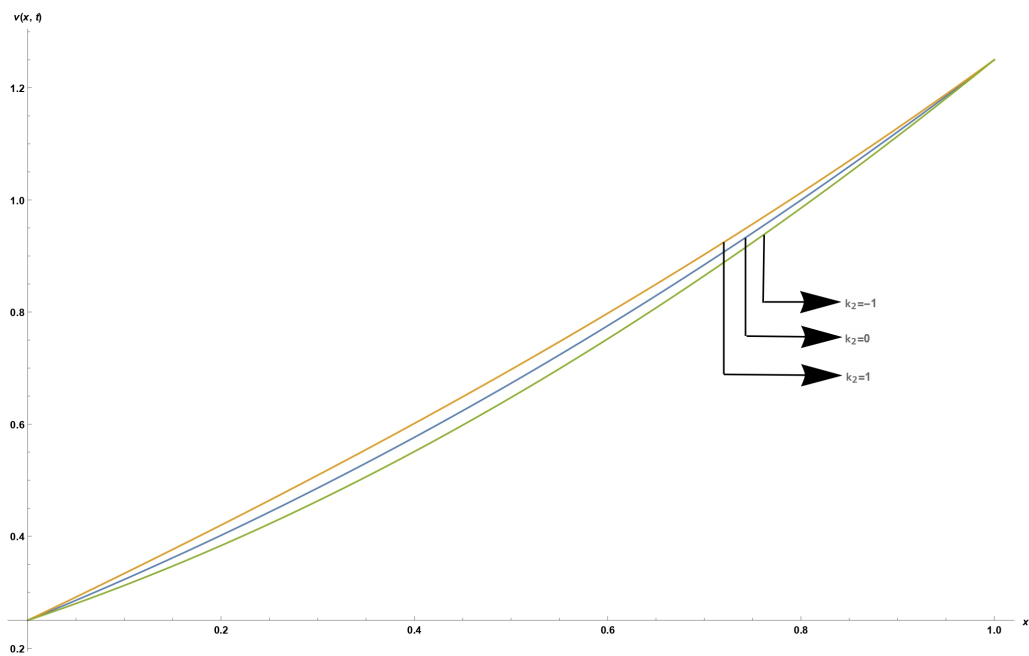


FIGURE 4.8: Plots of the solute concentration  $v(x, t)$  vs.  $x$  for different values of  $k_2$  for  $\alpha_2 = 0.8, \alpha_1 = 1$  at  $t = 0.5$ .

The effects of reaction terms on both solution profiles for various values of the fractional order time derivatives are found for different particular cases. It is seen that the solution

profiles are decreased as the system advances towards fractional order from standard order. It is also seen from the figures that damping are found due the presence of sink terms ( $k_1 = k_2 = -1$ ) as compared to the source terms ( $k_1 = k_2 = 1$ ). Figs. 4.7-4.8 reveal that it consumes less time for the stabilization of the probability density functions  $u(x, t)$  and  $v(x, t)$  at  $t = 0.5$  for the case  $\alpha_1 = \alpha_2 = 0.8$  due to the presence of sink terms  $k_1 = k_2 = -1$  as compared to the case of  $k_1 = k_2 = 0$  and also due to presence of source terms  $k_1 = k_2 = 1$ , which clearly shows that physical importance of the presence of sink term for the enhancement of stability region for both the solute species.

## 4.7 Conclusions

In this chapter, a more efficient numerical scheme has been introduced adopting Laguerre polynomial algorithm to find the approximate solution of a system of multi-term coupled PDEs. The author has tested the particular case of concerned model viz., system of coupled Burgers' equations to validate the higher accuracy and efficiency of the proposed method. This chapter has achieved three significant goals. First one signifies the exhibition of super-linearly convergence rate of the proposed method for various fractional order derivatives for solute species  $u(x, t)$  and  $v(x, t)$ . Second one is the demonstration of pictorial presentations of the nature and behaviour of the solution profiles due to the presence of reaction terms for different particular cases for both solute species with respect to column length at  $t = 0.5$ . The third one is the graphical presentations of the damping nature of both solute concentrations when the system approaches towards fractional order from standard order for conservative and non-conservative cases.